NON-LINEAR UNSTEADY AERODYNAMICS APPLICATION FOR AIRLINER FLUTTER RESEARCH

Chuban A.V.[1], Chuban V.D.[2]

[1] Design-Engineer, JSC Irkut Corporation
68, Leningradskiy prospect, Moscow, Russian Federation, 125315
andrey.chubani@irkut.com

[2] Head of Loads and Aeroelasticity Department, JSC Irkut Corporation
68, Leningradskiy prospect, Moscow, Russian Federation, 125315
vitaliy.chubani@irkut.com

Keywords: non-linear transonic aerodynamics, flutter calculation method, approximation of unsteady aerodynamic coefficients.

Abstract: There has been considered the task of non-linear transonic aerodynamics module to be integrated in the program that allows to analyze frequency-domain flutter performance for different aircraft configurations. New aerodynamics block is based on rapid numerical integration of the Euler unsteady equation linearized on the steady solution. The algorithm used is based on the iterative coupling of non-viscous solution for external flow and solution for spatial compressible viscous boundary layer. Aerodynamic block performs calculation of unsteady aerodynamic flows for aircraft rigid motions and elastic vibration modes at several values of Strouchal numbers Sh = ωb/V, ω — angular frequency, b — mean aerodynamic chord, V — true airspeed.

The elastic beam model makes use of simplified panel aerodynamic configuration whereas aerodynamic block utilizes 3-D aircraft model. Interaction between flutter calculation program and aerodynamic block is carried out using interpolation of elastic beam model displacements and velocities on to the 3-D aerodynamic model grid nodes and inverse interpolation of aerodynamic forces on to the elastic beam model grid nodes. Values of the aerodynamic coefficients calculated for several Strouchal numbers are used as reference points for the development of the third order fractional interpolation for each aerodynamic coefficient. Use of aerodynamic coefficient frequency approximations allows to solve flutter equations in frequency domain as well as to determine dynamic system poles. Standard methods of poles trajectory plotting with zero-damping points tracing is applied to determine critical flutter parameters.

Using mathematical model of the next generation airliner as an example the comparison is made as to the new CFD block with well-known DLM method for aerodynamic coefficients, pressure distribution and flutter analysis results. The comparison illustrates that both methods gave almost identical results for subsonic flow, but for transonic flow the difference between methods is remarkable.

1 INTRODUCTION

Calculation of aircraft flutter during transonic flight is a very important task because transonic flight mode is the most continuous for the majority of passenger airliners, heavy transport aircraft and military aircraft. However, it is known that critical flutter speed is very often decreased during transonic flight.

Use of panel methods widely applied in unsteady aerodynamics, such as double lattice method (DLM) [1], does not allow to take into account nonlinearities related to airfoil thickness, angle of attack of airfoil, and appearance of local supersonic areas. This means that flutter calculation with use of panel methods at Mach numbers close to one may be considered approximate. In late 70s of the last century, a tremendous up-growth of the computer science started works on usage of computational fluid dynamics for analysis of unsteady flows around a complete aircraft. In the beginning, rather quick methods of numerical solution of transonic small perturbation [2, 3] and full-potential [4] equations were widely used. But simplifications accounted in those equations led to misidentification of location of shocks and their dynamics. Then algorithms appeared which allowed solving of more exact and resource-intensive Euler's equations [5-7], and Reynolds averaged Navier-Stokes equations [8-9]. The latter ones, which consider flow viscosity, provide accurate solutions for developed flow separations at aerodynamic surface, but still are rather complicated from computational standpoint [10]. During airliners’ cruise flight regimes there are no separations at all or separations are small and reattached, so that one may assume that Euler’s equations solution considering boundary layer effect will provide acceptable results.

This area is underdeveloped in Russia. Domestic program BLWF120 by O.V. Karas and V.E. Kovalev has been the first to provide a tool required to investigate transonic flutter. It is a possibility to relatively quickly calculate unsteady flow around a complete aircraft based on numerical integration of Euler’s equations considering boundary layer (iterative coupling method). The main goal of the study is implementation of BLWF 120 program as aerodynamic block into IMAD computing complex [11] that allows calculation of flutter performances within a frequency domain with use of unsteady aerodynamics. The article provides overview of operation of the programs used and their interaction, as well as comparison of unsteady aerodynamics results and flutter characteristics defined with use of DLM and BLWF120 program for the promising passenger airliner.

2 OVERVIEW OF STEADY AND UNSTEADY COMPUTATION ALGORITHMS USED IN BLWF PROGRAM

Table 1 below shows main differences between BLWF120 and DLM method that is widely used in IMAD.

Parameter	DLM	BLWF
Type of equation being solved	Linear	Non-linear
Equations used	Helmholtz wave equations without considering airflow viscosity	Euler’s equations linearized onto non-linear steady solution considering boundary layer effect
Strouhal[1] number limitation	≤ 3	No limitation

[1] Reduced frequency, see the definition in paragraph 3

Parameter	DLM	BLWF
Angle-of-attack limitation	Zero angle-of-attack	All the way to build-up of large non-attached separations
Mach number limitation	< 0.9	< 3
Airfoil modeling	Flat panels considering profile camber	Detailed consideration of airfoil geometrical characteristics
Fuselage and engine nacelles modeling	Mostly cruciform configuration	Accurate modeling of surface geometrical characteristics

Table 1: Main differences between DLM and BLWF computation methods

BLWF120 program provides the fast computation of unsteady aerodynamic derivatives of a complete aircraft based on linearization of unsteady Euler's equations near steady solution. Steady solution is calculated in BLWF 100 program [12] using numerical integration of the Euler steady equations by means of fast implicit method considering viscosity effect within the framework of viscous-inviscid coupling.

Important advantage of BLWF120 program which significantly simplifies unsteady aerodynamics calculation is use of overlapping computational grids method. The program automatically builds up local computational grids around each aircraft structural element (fuselage, wing, engine nacelle etc.). Typical local grids are shown in Figure 1. Flow parameters on grid outer boundaries are defined by interpolation of parameters calculated for adjacent elements grids.

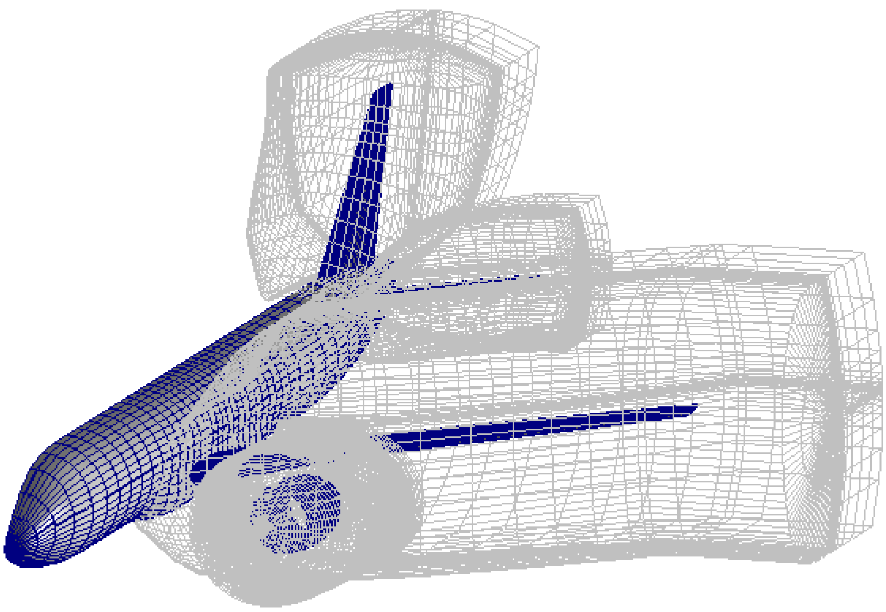

Figure 1: Aircraft aerodynamic model for BLWF calculation with local grids for separate aircraft structural elements

3 OVERVIEW OF BLWF AND IMAD INTERFACE

Numerical analysis of aircraft dynamic properties is performed in IMAD complex based on aircraft comprehensive mathematical model which includes finite element model of elastic aircraft with predefined stiffness and mass-inertia properties of the components, actuators dynamic stiffness, and aerodynamic model.

Upon completion of structure natural modes analysis, unsteady aerodynamic coefficients are calculated using BLWF for predefined list of Strouhal numbers Sh = 0, $0.5Sh_{max}$, Sh_{max}, $1.5Sh_{max}$, where Sh_{max} — representative Strouhal number defined by a user.

Interface between IMAD and BLWF includes three stages. At the first stage, IMAD exports file containing boundary conditions for specific aerodynamic flows in the form of translations or velocities in panel mesh nodes of a simplified aerodynamic model used in IMAD. For example, boundary conditions for an alpha-flow correspond to aircraft positioned at angle of attack.

At the second stage, steady and unsteady flows are calculated in BLWF100 and BLWF120 using detailed aerodynamic model predefined in BLWF input file. Boundary conditions in aerodynamic panel mesh nodes of IMAD model are translated into BLWF model using relative coordinates along the wingspan, wing chord, etc.

At the last stage, BLWF120 output file containing dimensionless pressure distribution among nodes of aircraft aerodynamic model for the whole list of aerodynamic flows and Strouhal numbers is imported into IMAD. Unsteady aerodynamic coefficients for the whole list of model natural modes are defined by numerical integration of a product of generalized displacements times unsteady aerodynamic pressures.

After that, parametrical study of flutter equations is performed, usually with flight altitude as a variable parameter and a constant Mach number. As flutter equations have unsteady aerodynamic coefficients as function of Strouhal number, these coefficients are defined in IMAD using approximation of earlier calculated aerodynamic coefficients for predefined set of Strouhal numbers [11]. Approximation is applied in the form of fractional rational function of the following nature: $C(Sh) = N(Sh)/D(Sh)$, where $N(Sh)$ and $D(Sh)$ are third order polynomial of Sh number. As referenced in [11], such approximation method allows keeping conventional methods of calculation of dynamic system poles due to increased number of equations. For this purpose, additional equations may be treated as equations defining delay in the aerodynamic forces behavior, i.e. their inherent nonstationarity. Thus calculated unsteady aerodynamic forces become the right hand side of the flutter equation. Then roots of the flutter equation are founded and dynamic system poles hodographs are plotted.

4 FLUTTER CALCULATION METHOD USING UNSTEADY AERODYNAMICS

Consider the approximation of unsteady aerodynamic coefficients for set of Strouhal numbers.

As situated above aerodynamic pressures are calculated for a set of boundary conditions and for a set of reduced frequencies which cover the required frequency range and include the zero value. Each particular flow may be denoted by an upper index k corresponding to a relevant kinematic parameter X_k and gives complex pressure distribution.

Knowing complex aerodynamic pressures allows one to calculate complex derivatives C_ℓ^k which are real quantities at zero value of the reduced frequency and become complex quantities otherwise; in addition, they depend on Mach number M and the reduced frequency. Here *l* denotes the component of the dimensionless aerodynamic forces and moments vector.

The reduced frequency may be defined using Strouhal number Sh as

$$\mathrm{Sh} = \Omega b/V$$

where Ω is the angular frequency, b — mean aerodynamic chord, V — airplane velocity.
It is convenient to introduce the complex reduced frequency

$$\mathbf{Sh} = sb/V \tag{1}$$

where $s = \sigma + i\Omega$ is the complex angular frequency or the Laplace operator, and i is the imaginary unit; when $s = i\Omega$, the complex reduced frequency becomes a purely imaginary value, $\mathbf{Sh} = i\mathrm{Sh}$.

The specified set of reduced frequencies may be represented as follows:

$$\mathrm{Sh}_0 = 0, \quad \mathrm{Sh}_1 = \frac{\Omega_1 b}{V}, \quad \mathrm{Sh}_2 = \frac{\Omega_2 b}{V}, \ldots$$

So, we may use $C_\ell^{k\,(m)}$ to denote a complex derivative C_ℓ^k for a reduced frequency Sh_m.

For numerical investigations we should restrict the set of reduced frequencies to a few terms. Let us consider aerodynamic derivatives approximation for three Strouhal numbers:

$$\mathrm{Sh}_0 = 0, \quad \mathrm{Sh}_1 = \frac{0.5\Omega_{\max} b}{V} = 0.5\mathrm{Sh}_{\max}, \quad \mathrm{Sh}_2 = \frac{\Omega_{\max} b}{V} = \mathrm{Sh}_{\max}$$

The next step is to approximate the complex derivatives by means of the analytical transfer function W (named also "filter"):

$$C_\ell^k(\mathbf{Sh}) = C_\ell^{k(0)} W(\mathbf{Sh}),$$

$$W(\mathbf{Sh}) = \frac{1 + \tau_{\ell 0}^k \mathbf{Sh} + (\tau_{\ell 1}^k)^2 \mathbf{Sh}^2}{1 + \tau_{\ell 2}^k \mathbf{Sh} + (\tau_{\ell 3}^k)^2 \mathbf{Sh}^2}$$

where real values $\tau_{\ell 0}^k$, $(\tau_{\ell 1}^k)^2$, $\tau_{\ell 2}^k$ and $(\tau_{\ell 3}^k)^2$ are dimensionless time constants.

The final representation of complex aerodynamic coefficients as functions of complex angular frequency is as follows:

$$C_\ell^k(s) = C_\ell^{k\,(0)} W(s), \tag{2}$$

$$W(s) = \frac{1 + T_{\ell 0}^k s + (T_{\ell 1}^k)^2 s^2}{1 + T_{\ell 2}^k s + (T_{\ell 3}^k)^2 s^2} \tag{3}$$

with real time constants

$$T_{\ell n}^k = \tau_{\ell n}^k \frac{b}{V}, \quad n = 0 - 3.$$

The transfer function W has the following properties:

1. It goes to a value of one as s goes to zero. So the correct values of aerodynamic derivatives are reached for quasi-steady state.
2. It goes to a finite real value of $(T_{\ell 1}^k / T_{\ell 3}^k)^2$ as s goes to infinity. The requirement for complex derivatives to be real conforms to the exact solution for dimensionless pressure C_p = 4/M for unit boundary condition at panel control point when $s = \infty$. This fact gives the principal difference in comparison with other known approaches.
3. It is a second-order transfer function capable of satisfactorily approximating the complex derivatives as functions of the complex angular frequency.
4. It can be used readily in both time and frequency domain analyses.
5. It represents a stable system. This is satisfied by requiring $T_{\ell 2}^k$ and $T_{\ell 3}^k$ to be positive.

The next step is the assumption that the index ℓ in $T_{\ell 2}^k$ and $T_{\ell 3}^k$ may be omitted, i.e.

$$T_{\ell 2}^k = T_2^k, \quad \mathrm{T}_{\ell 3}^k = T_3^k. \tag{4}$$

$$T_2^k > 0, \quad T_3^k > 0. \tag{5}$$

The relation (4) allows one to essentially reduce the total number of integrators and simplify the approach as shown below (in the "Frequency domain" subsection).

By using (2), (3), and (4) we may represent the generalized aerodynamic force as

$$C_\ell = C_{0\ell} + \frac{D_\ell^k + G_\ell^k s + F_\ell^k s^2}{1 + T_2^k s + (T_3^k)^2 s^2} X_k \tag{6}$$

where

$$\boldsymbol{D} = [D_\ell^k] = [C_\ell^{k(0)}], \quad \boldsymbol{G} = [G_\ell^k] = [C_\ell^{k(0)} T_{\ell 0}^k],$$
$$\boldsymbol{F} = [F_\ell^k] = [C_\ell^{k(0)} (T_{\ell 1}^k)^2]$$

note that the superindex (0) corresponds to the zero frequency.

The unknown vector $\boldsymbol{Z}$ with components

$$Z_k = \frac{1}{1 + T_2^k s + (T_3^k)^2 s^2} X_k$$

may be introduced to provide

$$(\boldsymbol{E} + s\boldsymbol{T}_2 + s^2 \boldsymbol{T}_3^2)\boldsymbol{Z} = \boldsymbol{X} \tag{7}$$

where $\boldsymbol{E}$ is the diagonal unit matrix and $\boldsymbol{T}_2 = \lceil T_2^k \rfloor$ and $\boldsymbol{T}_3 = \lceil T_3^k \rfloor$ are diagonal matrices. By introducing a new unknown vector

$$\boldsymbol{U} = s\boldsymbol{Z}, \tag{8}$$

eqn (7) may be re-written:

$$s\boldsymbol{U} = \boldsymbol{T}_3^{-2}(\boldsymbol{X} - \boldsymbol{Z} - \boldsymbol{T}_2\boldsymbol{U}). \tag{9}$$

Upon combining eqns (6), (8), and (9) it can be shown that

$$\begin{cases} \begin{bmatrix} \dot{\boldsymbol{Z}} \\ \dot{\boldsymbol{U}} \end{bmatrix} = \begin{bmatrix} \boldsymbol{0} & \boldsymbol{0} & \boldsymbol{E} \\ \boldsymbol{T}_3^{-2} & -\boldsymbol{T}_3^{-2} & -\boldsymbol{T}_3^{-2}\boldsymbol{T}_2 \end{bmatrix} \begin{bmatrix} \boldsymbol{X} \\ \boldsymbol{Z} \\ \boldsymbol{U} \end{bmatrix} \\ \boldsymbol{C} = \boldsymbol{C}_0 + \begin{bmatrix} \boldsymbol{F}\,\boldsymbol{T}_3^{-2} & \boldsymbol{D} - \boldsymbol{F}\,\boldsymbol{T}_3^{-2} & \boldsymbol{G} - \boldsymbol{F}\,\boldsymbol{T}_3^{-2}\boldsymbol{T} \end{bmatrix} \begin{bmatrix} \boldsymbol{X} \\ \boldsymbol{Z} \\ \boldsymbol{U} \end{bmatrix} \end{cases} \tag{10}$$

If the process is quasi-steady, then $\boldsymbol{U} \approx 0$, $\boldsymbol{Z} \approx \boldsymbol{X}$ and $\boldsymbol{C} \approx \boldsymbol{C}_0 + \boldsymbol{DX}$, i.e., the aerodynamic forces correspond exactly to zero reduced frequency. In the general case, the time history of aerodynamic forces has time lags relative to vector X time history. Generally, eqn (10) can immediately be utilized to compute unsteady aerodynamic forces. The above condition (4) made it possible to derive a rather simple form of these equations, as well as notably decrease the order of the system; this fact is very important in practice. Let us consider application of the expression to the unsteady problem in two important situations for frequency and time domain analyses.

4.1 Frequency domain. Flutter analysis

The typical equation used in the quasi-steady flutter problem may be written as follows:

$$\boldsymbol{M}\dot{\boldsymbol{X}} = \boldsymbol{A}_0\boldsymbol{X} + \boldsymbol{DX} \tag{11}$$

where the last term represents quasi-steady aerodynamic forces. Matrices $\boldsymbol{M}$ and $\boldsymbol{A}_0$ are known. Here, $\boldsymbol{M}$ may be interpreted as the generalized mass matrix, and $\boldsymbol{A}_0$ is the generalized matrix allowing for structural damping forces and stiffness.

Using eqns (6), (10), and (11) the equations for unsteady flutter may be written as,

$$\begin{cases} \boldsymbol{M}\dot{\boldsymbol{X}} = \boldsymbol{A}_0 + \boldsymbol{DZ} + \boldsymbol{GU} + \boldsymbol{F}\dot{\boldsymbol{U}} \\ \dot{\boldsymbol{Z}} = \boldsymbol{U} \\ \dot{\boldsymbol{U}} = \boldsymbol{T}_3^{-2}\boldsymbol{X} - \boldsymbol{T}_3^{-2}\boldsymbol{Z} - \boldsymbol{T}_3^{-2}\boldsymbol{T}_0\boldsymbol{U} \end{cases}$$

or, in matrix notation,

$$\begin{bmatrix} \boldsymbol{M} & \boldsymbol{0} & -\boldsymbol{F} \\ \boldsymbol{0} & \boldsymbol{E} & \boldsymbol{0} \\ \boldsymbol{0} & \boldsymbol{0} & \boldsymbol{E} \end{bmatrix} \begin{bmatrix} \dot{\boldsymbol{X}} \\ \dot{\boldsymbol{Z}} \\ \dot{\boldsymbol{U}} \end{bmatrix} = \begin{bmatrix} \boldsymbol{A}_0 & \boldsymbol{D} & \boldsymbol{G} \\ \boldsymbol{0} & \boldsymbol{0} & \boldsymbol{E} \\ \boldsymbol{T}_3^{-2} & -\boldsymbol{T}_3^{-2} & -\boldsymbol{T}_3^{-2}\boldsymbol{T}_2 \end{bmatrix} \begin{bmatrix} \boldsymbol{X} \\ \boldsymbol{Z} \\ \boldsymbol{U} \end{bmatrix} \tag{12}$$

By introducing the new unknown vector

$$\boldsymbol{V} = \boldsymbol{Z} - \boldsymbol{X}$$

eqn (12) may be represented finally as

$$\begin{bmatrix} \boldsymbol{M} & \boldsymbol{0} & \boldsymbol{0} \\ \underline{\boldsymbol{E}} & \boldsymbol{E} & \boldsymbol{0} \\ \boldsymbol{0} & \boldsymbol{0} & \boldsymbol{E} \end{bmatrix} \begin{bmatrix} \dot{\boldsymbol{X}} \\ \dot{\boldsymbol{V}} \\ \dot{\boldsymbol{U}} \end{bmatrix} = \begin{bmatrix} \boldsymbol{A}_0 + \boldsymbol{D} & \underline{(\boldsymbol{D} - \boldsymbol{F}\,\boldsymbol{T}_3^{-2})} & \underline{(\boldsymbol{G} - \boldsymbol{F}\,\boldsymbol{T}_3^{-2}\boldsymbol{T}_2)} \\ \boldsymbol{0} & \boldsymbol{0} & \boldsymbol{E} \\ \boldsymbol{0} & -\boldsymbol{T}_3^{-2} & -\boldsymbol{T}_3^{-2}\boldsymbol{T}_2 \end{bmatrix} \begin{bmatrix} \boldsymbol{X} \\ \boldsymbol{V} \\ \boldsymbol{U} \end{bmatrix}.$$

If the process is quasi-steady one, then $\boldsymbol{U} \approx \boldsymbol{V} \approx 0$ and the underlined terms of the equation may be ignored, so the flutter equation coincides with eqn (11). It is evident that the "price" of unsteady solution is three times the system dimensionality. Again, we see that (4) greatly decreases the state vector dimensionality in the flutter analysis for unsteady problem.

4.2 Time domain. Transient response analysis

For this kind of analysis the system (10) must be integrated simultaneously – both the basic equations of elastic body motion and the equations of the onboard control system with sensors and actuators.

The "price" of the unsteady approach is approximately three times the number of integrators.

So the approach makes it possible to represent aerodynamic forces in both frequency and time domains and can be used to analyze any non-stationary motion of airplane. Eqn (3) can be treated as a second-order filter with unknown parameters $T_{\ell 0}^{k}, T_{\ell 1}^{k}, T_{2}^{k}, T_{3}^{k}$.

Obviously, eqn (2) should give correct values of complex derivatives in the case of harmonic oscillations ($s = i\Omega$). This condition is the basis of a numerical algorithm for determining unknown parameters of all filters. Thus, the expressions (2) are required to approximate the values known at reduced frequencies of $0.5\mathrm{Sh}_{max}$ and Sh_{max}.

The cost function is defined as the total square deviation between values of aerodynamic derivatives obtained by using the DLM and the corresponding values of the transfer functions (3) at reduced frequencies of $0.5\mathrm{Sh}_{max}$ and Sh_{max}. In this case the objective function argument is the set of time constants $T_{\ell n}^{k}$, $n = 0 – 3$.

The numerical procedure developed is based on discrete multi-level global minimization of the corresponding cost function with restrictions (5).

5 MATHEMATICAL MODEL DESCRIPTION

Elastic aircraft mathematical model represents a set of beam sub-structures divided into finite elements. Sub-structures displacement compatibility in attachment points is provided by means of common springs. Model general layout including sub-structures attachment points is shown in Figure 2.

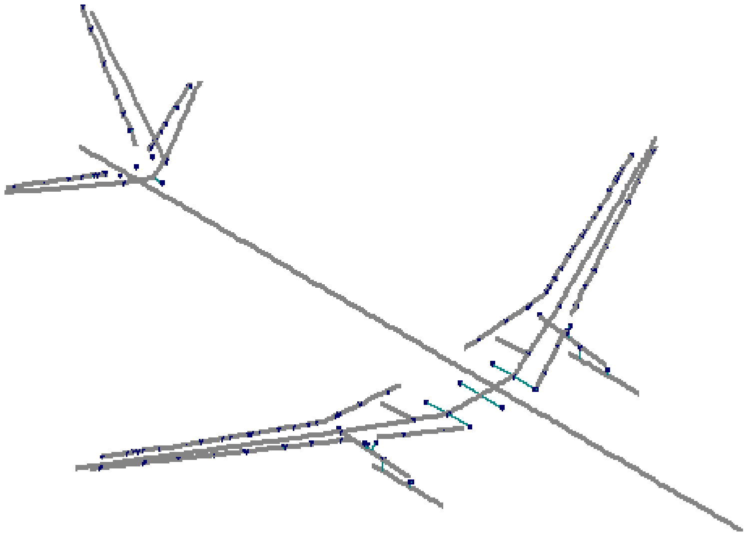

Figure 2: General layout of aircraft beam structure including sub-structures attachment points

For the purpose of DLM calculation, aircraft aerodynamic model is usually defined using thin lifting panels, the geometry of which corresponds to aircraft sub-structures planform view. Fuselage and engine aerodynamic models defined using crucified configuration also include vertically located panels (see Figure 3).

As opposed to DLM, BLWF allows to consider actual geometric shapes of sub-structures such as fuselage and engine (see Figure 4). To create corresponding aerodynamic models with solid bodies, IMAD complex has additional capability to import aircraft geometric data in accordance with BLWF input file structure. Besides, while DLM calculations only consider mean curvature of lifting surfaces, BLWF flow calculations consider actual profile of the wing, stabilizer etc. That said, differential pressure distribution shape having zero at the leading edge with further pressure surge requires much more accurate definition of the computational mesh.

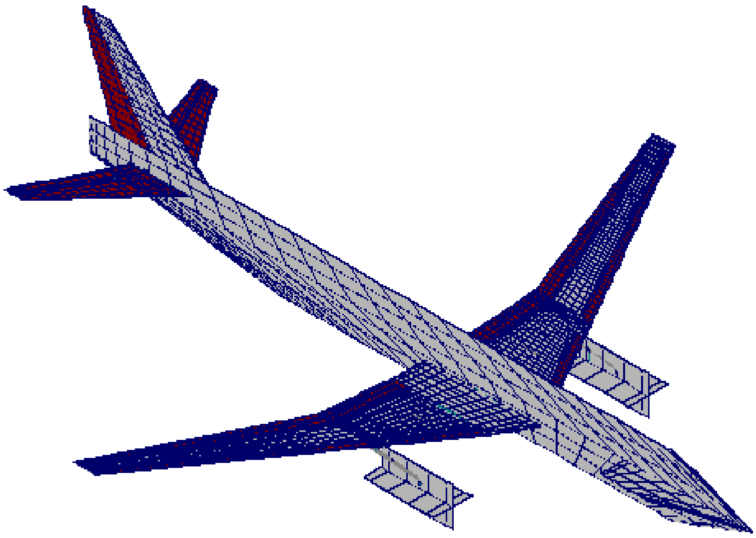

Figure 3: Aircraft aerodynamic model used for DLM calculations

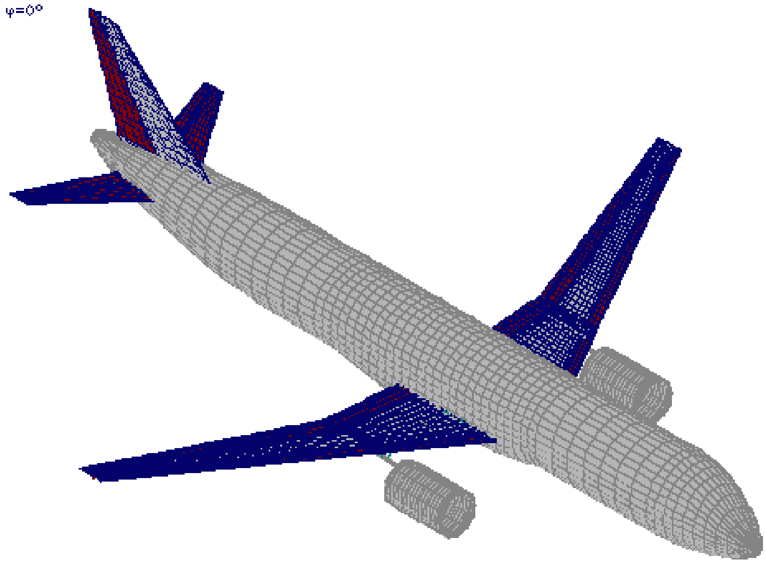

Figure 4: Aircraft aerodynamic model used for BLWF calculations

6 FLUTTER CALCULATION RESULTS

Comparison of BLWF and DLM results of critical speed calculation for two types of symmetrical flutter is described below. Critical speed values are shown in relative numbers.

6.1 Horizontal tail symmetrical flutter

Horizontal tail symmetrical flutter appears when there is interaction of elevator rotation, elevator first torsion mode and elevator second bending mode. Calculated critical flutter speed versus Mach number M curves for both numerical methods are shown in Figure 5. DLM shows gradual increase of critical flutter speed up to M = 0.85, while BLWF demonstrates sharp decrease of critical flutter speed down to M = 0.82 – 0.85. At cruise speed *M* = 0.82, critical flutter speed is almost identical.

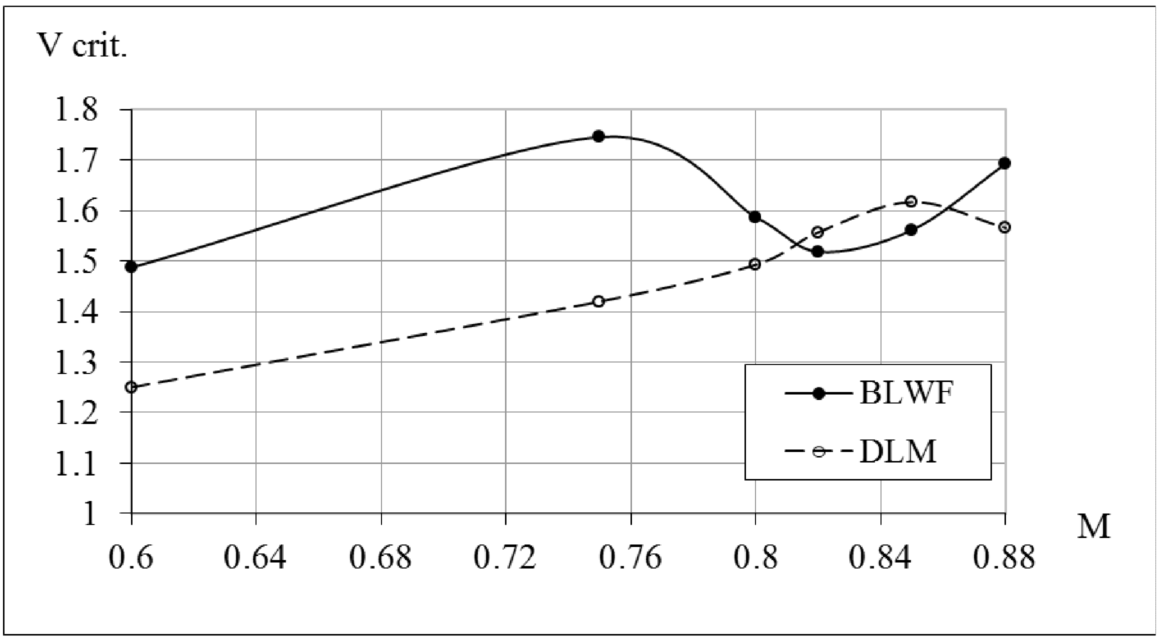

Figure 1: Critical speed of horizontal tail symmetrical flutter versus Mach number

6.2 Wing symmetrical flutter

Wing symmetrical flutter appears when there is interaction of wing first bending mode and wing first torsion mode. DLM calculation shows gradual decrease of critical flutter speed as long as Mach number increases, while for BLWF critical flutter speed goes down to M = 0.82 and then increases (see Figure 6). At cruise speed M = 0.82, critical flutter speed is almost identical.

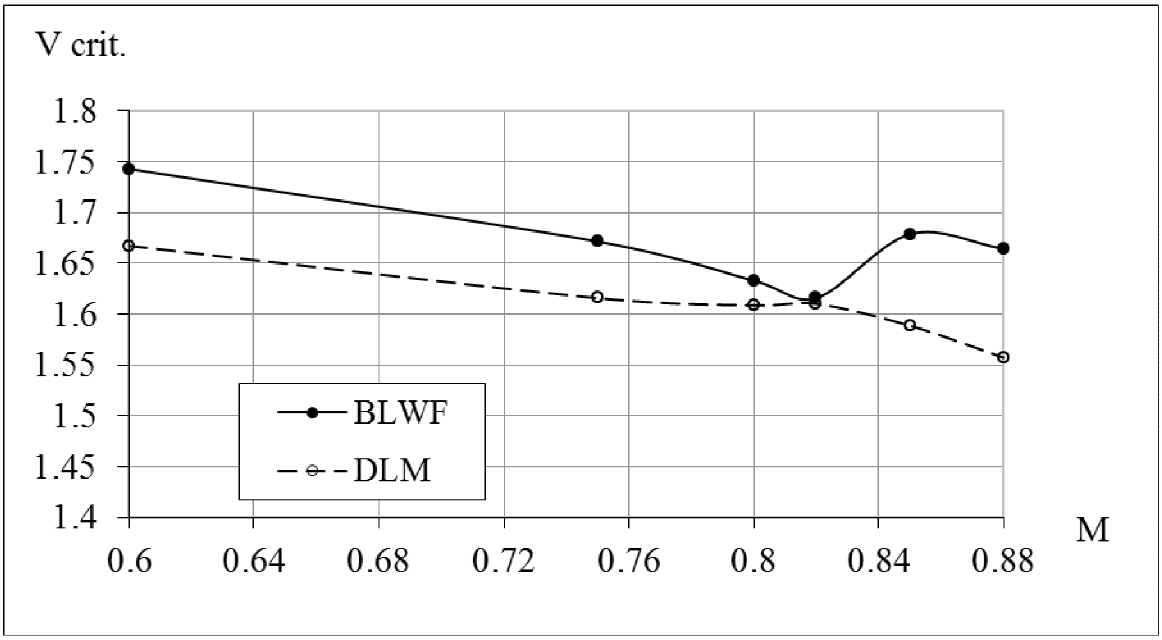

Figure 2: Critical speed of wing symmetrical flutter versus Mach number

7 CONCLUSION

A new aerodynamic module based on the non-linear transonic aerodynamic program BLWF120 has been added to IMAD complex. The upgraded IMAD code has become suitable for aircraft flutter calculation at any flight stage, including transonic flight. A case study of results obtained in DLM and BLWF120 aerodynamic modules has been performed using flutter characteristics analysis of the promising passenger aircraft as example.

8 REFERENCES

[1] Albano Y. E., Rodden W. P., A doublet-lattice method for calculating lift distribution on oscillating surfaces in subsonic flow, *AIAA Journal, Vol. 7, No. 2*, 1969;

[2] Borland C. J., Rizzetta D. P., Nonlinear transonic flutter analysis, *AIAA Journal, Vol. 20, No. 11*, 1982, pp. 1606-1615;

[3] Batina J. T., Seidel D. A., Bland S. R., Bennett R. M., Unsteady transonic flow calculations for realistic aircraft configurations, *Journal of Aircraft, Vol. 26, No. 1*, 1989, pp. 21-28;

[4] Ide H., Shankar V. J., Unsteady full potential aeroelastic computations for flexible configurations, *AIAA Paper 87-1238*, June 1987;

[5] Guruswamy G. P., Time-accurate unsteady aerodynamic and aeroelastic calculations of wings using Euler equations, *AIAA Paper 88-2281*, April 1988;

[6] Rausch R. D., Batina J. T., Yang T. Y., Euler flutter analysis of airfoils using unstructured dynamic meshes, *AIAA Paper 89-1384,* April 1989;

[7] Batina J. T, Unsteady Euler airfoil solutions using unstructured dynamic meshes, *AIAA Journal, Vol. 28, No. 8,* 1990, pp. 1381-1388;

[8] Guruswamy G. P., Vortical flow computations on swept flexible wings using Navier-Stokes equations, *AIAA Paper 89-1183*, April 1989;

[9] Guruswamy G. P., Vortical flow computations on a flexible blended wing-body configuration, *AIAA Paper 91-1013*, April 1991;

[10] Bendiksen O. O., Review of unsteady transonic aerodynamics: theory and applications, *IFASD-2009-062*, June 2009;

[11] Chuban, V. D., Ivanteyev, V. I., Chudayev, B. J., Avdeyev, E. P., Shvilkin, V. A. Numerical simulation of flutter validated by flight-test data for TU-204 aircraft, *Computers and Structures, Vol. 80*, 2002, pp. 2551-2563;

[12] Kovalev V.E., Karas O.V., Computation of a transonic airfoil flow considering viscous effects and thin separated regions. *Rech.Aerosp. N1991-1*.

COPYRIGHT STATEMENT

The authors confirm that they, and/or their company or organization, hold copyright on all of the original material included in this paper. The authors also confirm that they have obtained permission, from the copyright holder of any third party material included in this paper, to publish it as part of their paper. The authors confirm that they give permission, or have obtained permission from the copyright holder of this paper, for the publication and distribution of this paper as part of the IFASD 2015 proceedings or as individual off-prints from the proceedings.